

Article

Solvent Deuterium Oxide Isotope Effects on the Reactions of Organophosphorylated Acetylcholinesterase[†]

Terrone L. Rosenberry^{ID}

Mayo Clinic College of Medicine, Departments of Neuroscience and Pharmacology, Jacksonville, FL 32224, USA; rosenberry@mayo.edu ; Tel.: +1-904-953-7375; Fax: +1-904-953-7370

[†] This manuscript was given as an oral presentation on December 9, 2019 at the 16th Symposium on Cholinergic Mechanisms in Rehovot, Israel.

Academic Editor: Zrinka Kovarik

Received: 1 August 2020; Accepted: 17 September 2020; Published: 25 September 2020



Abstract: Organophosphates (OPs) are esters of substituted phosphates, phosphonates or phosphoramidates that react with acetylcholinesterase (AChE) by initially transferring the organophosphityl group to a serine residue in the enzyme active site, concomitant with loss of an alcohol or halide leaving group. With substituted phosphates, this transfer is followed by relatively slow hydrolysis of the organophosphoryl AChE, or dephosphorylation, that is often accompanied by an aging reaction that renders the enzyme irreversibly inactivated. Aging is a dealkylation that converts the phosphate triester to a diester. OPs are very effective AChE inhibitors and have been developed as insecticides and chemical warfare agents. We examined three reactions of two organophosphoryl AChEs, dimethyl- and diethylphosphorylated AChE, by comparing rate constants and solvent deuterium oxide isotope effects for hydrolysis, aging and oxime reactivation with pralidoxime (2-PAM). Our study was motivated (1) by a published x-ray crystal structure of diethylphosphorylated AChE, which showed severe distortion of the active site that was restored by the binding of pralidoxime, and (2) by published isotope effects for decarbamylation that decreased from 2.8 for *N*-monomethylcarbamoyl AChE to 1.1 for *N,N*-diethylcarbamoyl AChE. We previously reconciled these results by proposing a shift in the rate-limiting step from proton transfer for the small carbamoyl group to a likely conformational change in the distorted active site of the large carbamoyl enzyme. This proposal was tested but was not supported in this report. The smaller dimethylphosphoryl AChE and the larger diethylphosphoryl AChE gave similar isotope effects for both oxime reactivation and hydrolysis, and the isotope effect values of about two indicated that proton transfer was rate limiting for both reactions.

Keywords: acetylcholinesterase; paraoxon; dephosphorylation; reactivation; D₂O isotope

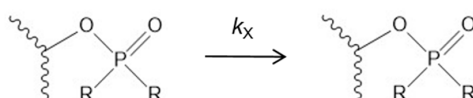
1. Introduction

Acetylcholinesterase (AChE) catalyzes the hydrolysis of the neurotransmitter acetylcholine, and rapid hydrolysis of this ester is essential for normal cholinergic synaptic transmission. Acetylcholine hydrolysis proceeds by transfer of the acetyl group to the active site serine of AChE followed by hydrolysis, or deacetylation, of the acetyl enzyme, and both steps occur on a timescale of microseconds [1]. Other ester substrates of AChE proceed through a similar two-step catalytic pathway (Scheme 1). However, the pathways for the esters in Scheme 1 differ from that of acetylcholine in that these esters initially form a detectable reversible equilibrium complex with AChE with a dissociation constant, K_D , before transfer of their carbamoyl or organophosphoryl groups (here referred to as acyl groups) to the active site serine to give carbamoyl or phosphoryl intermediates. This complex is an intermediate with acetylthiocholine but is not detectable, as explained in Equation (1) below. While the hydrolysis of the carbamoyl or organophosphoryl intermediates involves transfer of their

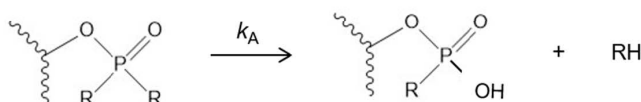
2. Results

The primary objectives of this paper are to obtain the solvent D₂O isotope effects for three of four reactions that involve organophosphorylated AChEs. The four reactions are outlined in Scheme 2, and the isotope effects are shown in Table 1 below. Because the determination of solvent D₂O isotope effects requires accuracy and precision, an emphasis is placed on protocols for rate constant measurement. The isotope effects obtained are then compared to those previously measured for carbamoylated AChEs, and differences among them are interpreted in the context of X-ray crystal structures determined for organophosphorylated AChEs like those shown in Figure 2.

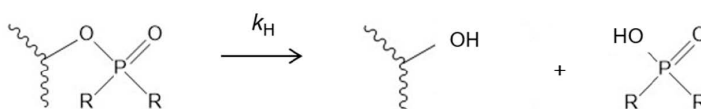
a) Denaturation



b) Aging



c) Hydrolysis



d) Oxime Reactivation



Scheme 2. Four reactions of organophosphorylated AChE (a–d). The alcohol RH, the phosphate diester R₂P(O)OH, and the phosphate triester R₂(oxime)P(O) are the products released during the aging, hydrolysis and reactivation reactions, respectively.

Protocols to measure the rate constants of the reactions of organophosphorylated AChEs in Scheme 2, in both H₂O and D₂O, are outlined in the Materials and Methods, and representative reactions are illustrated in Figures 3–5 below.

2.1. Denaturation Rate Constants k_X for Organophosphorylated AChE

Before the rate constants for reactions b, c and d in Scheme 2 can be determined, the loss of AChE activity arising from enzyme denaturation must be taken into consideration. The reaction denoted denaturation in Scheme 2a was detected with control AChE and with fully reactivated AChE in the absence of OPs. Bovine serum albumen (BSA) was added to the assay solution to stabilize the AChE, but the enzyme still showed a slow loss of activity with a rate constant k_X that (1) in some cases was close enough to the aging rate constant k_A and the hydrolysis rate constant k_H to require inclusion in the analytical equations and (2) was stabilized by 2-PAM and thus depended on the concentration of 2-PAM. Individual measurements of k_X ranged from 2–7 × 10^{−5} min^{−1} and are illustrated in Figures 4 and 5A below. The same denaturation constant k_X was assumed to apply to free and organophosphorylated AChE.

2.2. Aging Rate Constants k_A for Organophosphorylated AChE

The fact that organophosphorylated AChE can undergo multiple reactions (Scheme 2) required a sequential approach to obtaining the rate constants for these reactions. Fitting some of the data here to equations required preliminary estimates of some rate constants that were refined in the fitting of later data. The aging reaction in Scheme 2b is the loss of an alkoxy group attached to the phosphorus atom [14]. The resulting phosphate diester that remains covalently linked to AChE is an extremely stable inactive enzyme form that cannot be reactivated by oxime (Figure 3). The protocol we used to measure the aging rate constants k_A is indicated in the Figure 3 legend. We followed this protocol to obtain our best estimates of k_A in both H₂O and D₂O. AChE was maintained in a fully organophosphorylated form for various times t_{aged} , after which it was diluted into a high concentration of 2-PAM to rapidly reactivate all of the enzyme that had not been aged. Figure 3A demonstrates that, with reasonable initial estimates of k_X , k_A , k_H , and k_r , 2-PAM reactivation proceeds rapidly. Fitting confirmed that all values of v measured after the initial value near $t = 0$ essentially corresponded to the final value of v , denoted v_F . Plots of these v_F against t_{aged} could be analyzed with Equation (3) as shown in Figure 3B to give values of k_A presented in Table 1.

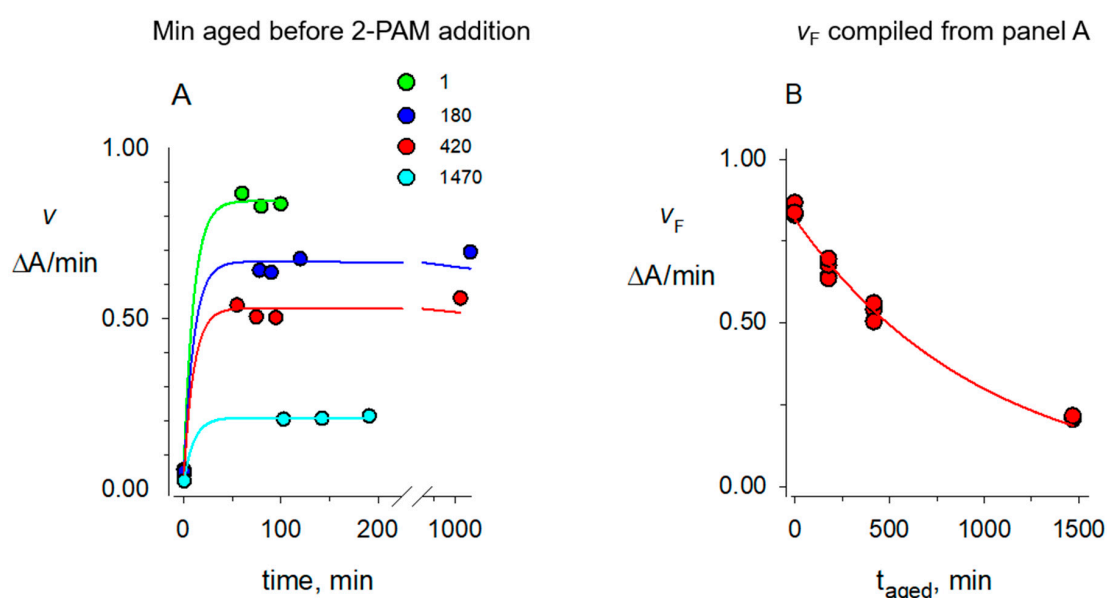


Figure 3. Aging of dimethylphosphorylated AChE in H₂O. A mixture of 2.4 μM paraoxon methyl (OP) and 0.5 μM AChE in 100 mM sodium phosphate and 0.1% BSA (pH 8.0) was incubated for 60 min at 25 °C. The incubation was then aged for the various times indicated before addition of 2-PAM, with the earliest addition of 2-PAM designated as $t_{\text{aged}} = 0$. To ensure that the OP remained in excess during aging, additional OP was added (1.7 μM at t_{aged} 5 and 185 min and 3.6 μM at t_{aged} 425 min). At the indicated t_{aged} of 1, 180, 420 and 1470 min, portions of the aged reaction were diluted 24-fold into 1.0 mM 2-PAM. (A) Aliquots (30 μL) of each dilution were assayed as indicated in the Materials and Methods at the times indicated on the x-axis. Assay values v were fit to Equation (2), with the indicated t_{aged} fixed. Fixed initial estimates (min^{-1} for k values) of $k_X = 2.5 \times 10^{-5}$, $k_H = 6.5 \times 10^{-3}$, $k_r = 9 \times 10^{-2}$ and $k_A = 2 \times 10^{-3}$ gave fitted $E_{\text{tot}} = 0.86 \Delta A/\text{min}$ (green line); this E_{tot} was then fixed along with the same values of k_X , k_H , and k_r to fit $k_A = 1\text{--}2 \times 10^{-3}$ and $E_0 = 0.01\text{--}0.02 \Delta A/\text{min}$ (blue, red, and cyan lines). Values for times after the initial time point were observed to correspond to the final value of v , denoted v_F , in this equation. (B) Assay values corresponding to v_F in panel A were analyzed with Equation (3) with a fixed $k_X = 2.5 \times 10^{-5} \text{ min}^{-1}$ to give $E_{\text{tot}} = 0.82 \Delta A/\text{min}$ and a k_A value of $(980 + 60) \times 10^{-6} \text{ min}^{-1}$ included in Table 1.

2.3. Hydrolysis Rate Constants k_H for Organophosphorylated AChE

The hydrolysis rate constants k_H were measured in H₂O and D₂O with the protocol in the Figure 4 legend. AChE was organophosphorylated and diluted with or without 200 μ M 2-PAM. Assay values v from the dilution with 2-PAM rapidly reached maximums and were analyzed with Equation (2) to determine E_{tot} . This value of E_{tot} was then fixed in Equation (2) to fit the values of v from the dilution without 2-PAM to obtain k_H (Figure 4).

In contrast to the protocol for the aging reaction in Figure 3A, where a slight excess of OP during preincubation was rapidly turned over by dilution into a high concentration of 2-PAM, the hydrolysis reaction was defined in the absence of 2-PAM and its time course was sensitive to any excess of OP. An excess was indicated by an E_0 close to zero and by a lag in the increase in v with time. Centrifugation through a spin column was employed to minimize unreacted OP but, in addition, the stoichiometry of AChE and OP was set close to one and the incubation time was limited to insure that, in most cases, E_0 was significantly greater than zero. However, this was not the case in Figure 4, where E_0 approached zero.

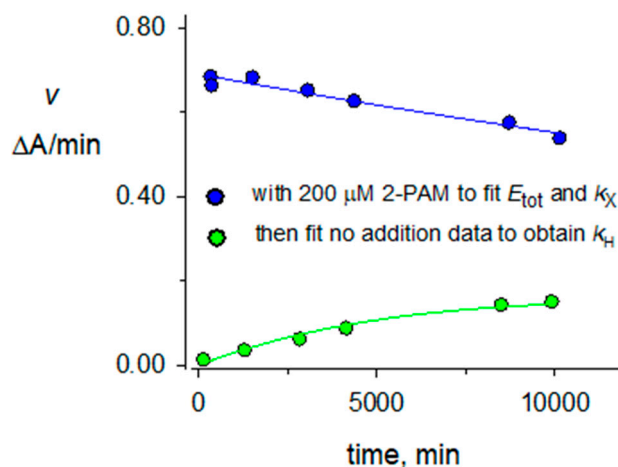


Figure 4. Denaturation and hydrolysis of diethylphosphorylated AChE in D₂O. A mixture of 2.0 μ M paraoxon and 1.4 μ M AChE in 100 mM sodium phosphate and 0.1% BSA (buffer) in D₂O (pH 8.0) was incubated for 70 min at 25 °C. A 4-fold excess of buffer in D₂O was added, and 200 μ L was applied to a 0.5 mL Sephadex G50 spin column (Fisher) that had been prewashed four times in buffer in D₂O and centrifuged at 1000 \times g for 1 min. The eluent was cooled to 4 °C, and 60 μ L was added either to 640 μ L of buffer in D₂O at 25 °C or 640 μ L of the same buffer with 2-PAM (to 200 μ M) at 25 °C. Aliquots (30 μ L) were assayed as in Figure 3 at the times indicated on the x-axis. Assay values v for the solution containing 2-PAM (blue points that correspond to enzyme denaturation) were first fit to Equation (2) with t_{aged} set to 0 and fixed initial estimates (min^{-1} for k values) of $k_A = 4 \times 10^{-5}$, $k_H = 4 \times 10^{-5}$, $k_r = 2 \times 10^{-2}$ and $E_0 = 0.01 \Delta\text{A}/\text{min}$ to obtain $k_\chi = 2.2 \times 10^{-5}$ and $E_{tot} = 0.69 \Delta\text{A}/\text{min}$. These values of t_{aged} , k_A , and E_{tot} along with $k_\chi = 4 \times 10^{-5}$ and $k_r = 0$ were then fixed into Equation (2) to fit the assay values v for the solution without 2-PAM (green points that reflect enzyme denaturation and diethylphosphorylated enzyme hydrolysis). This fitting gave $E_0 = 0.003 \Delta\text{A}/\text{min}$ and a k_H value of $(47 + 3) \times 10^{-6} \text{min}^{-1}$ included in Table 1.

2.4. 2-PAM Reactivation Rate Constants k_R for Organophosphorylated AChE

The reactivation rate constants k_r depend on the concentration of 2-PAM, but at the 2-PAM concentrations employed here they were considerably larger than rate constants for denaturation, aging and hydrolysis described above. Nevertheless, the determination of accurate solvent D₂O isotope effects required inclusion of these smaller rate constants in Equation (2). The protocol for obtaining values of k_r is shown in Figure 5A. A rapid increase in assay values v was observed on adding organophosphorylated AChE to 2-PAM, followed by a much slower decrease in v that we

attributed to enzyme denaturation. The much longer slow decrease dominated the fitting procedure when the entire time course was analyzed, so fitting was divided into two steps. In the first step only the denaturation rate constant k_X was retained, and it showed a clear decrease in value at higher 2-PAM concentrations (Figure 5A) as noted above. The second fitting step retained the value of k_X from the first step as an additional fixed variable, and k_r was fitted from the initial increase in v (Figure 5A). Values of k_r obtained at different 2-PAM concentrations were then analyzed according to Equation (4) to obtain the maximum reactivation rate constant k_R at concentrations of 2-PAM that saturated the organophosphorylated enzyme (Figure 5B).

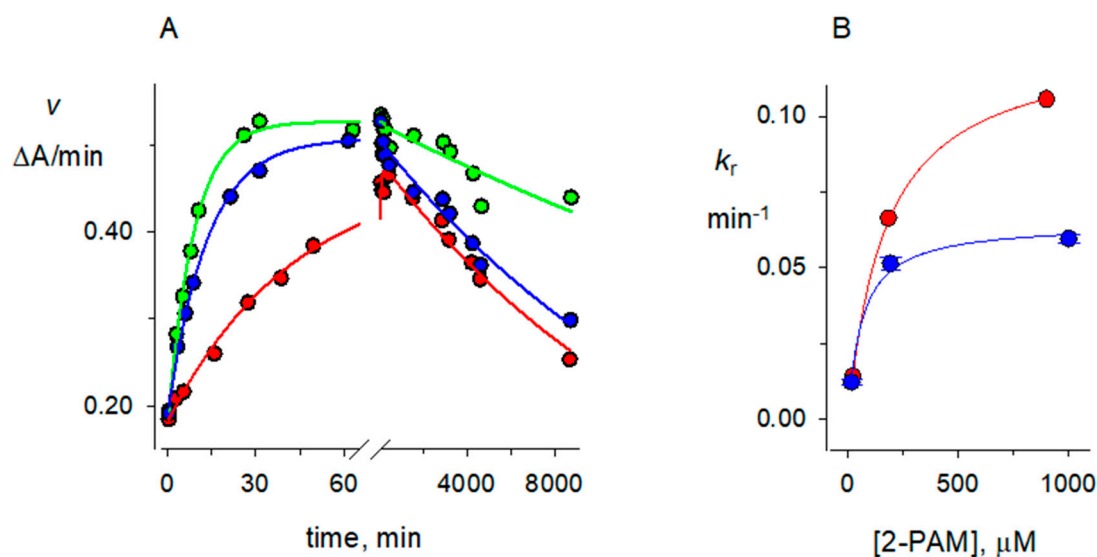


Figure 5. 2-PAM reactivation of dimethylphosphorylated AChE in H₂O. A mixture of 1.6 μM paraoxon methyl and 1.5 μM AChE in 100 mM sodium phosphate and 0.1% BSA (buffer) in H₂O (pH 8.0) was incubated for 30 min at 25 °C. A 2.5-fold excess of buffer in H₂O was added, and 100 μL was applied to a 0.5 mL spin column that had been prewashed four times in buffer in H₂O and centrifuged at 1000× *g* for 1 min. The eluent was added to 215 μL of buffer in H₂O and cooled to 4 °C, and 100 μL aliquots were added at time zero to 700 μL of buffer in H₂O containing final concentrations of 905, 185, or 24 μM 2-PAM at 25 °C. (A) Aliquots (30 μL) were assayed as indicated in Figure 3 at the times indicated on the *x*-axis. Assay values v for the solutions containing 905 μM (green points), 185 μM (blue points) or 24 μM 2-PAM (red points) were analyzed with Equation (2) in two steps, with t_{aged} set to 0 and k_A and k_H fixed at $2 \times 10^{-3} \text{ min}^{-1}$ and $6 \times 10^{-3} \text{ min}^{-1}$, respectively, and k_r , k_X , E_{tot} , and E_0 as fitted variables. In the first step, points over the entire 8800-min time course were fitted to obtain k_X (in min^{-1}) = 2.5×10^{-5} (green points), 6.3×10^{-5} (blue points), and 7.0×10^{-5} (red points). These k_X were then fixed along with k_A and k_H in the second step in which time courses of 250 to 450 min were fitted to give more precise values of k_r . (B) Values of k_r from the second fitting step in panel A were then fitted to Equation (4) to obtain values of k_R (12.5 ± 0.2) $\times 10^{-2} \text{ min}^{-1}$ included in Table 1. The corresponding fit of k_r values obtained in D₂O is also shown. Fitted values of K_P were 170 μM in H₂O and 90 μM in D₂O. Error values typical of k_r for both H₂O and D₂O data sets are shown with the D₂O data points.

2.5. Accuracy of Rate Constants for Reactions of Organophosphorylated hAChE

In addition to the rate constants given in Table 1, we also determined k_X values in the absence of 2-PAM in H₂O ($(53 \pm 7) \times 10^{-6} \text{ min}^{-1}$, $n = 7$) and in D₂O ($(41 \pm 14) \times 10^{-6} \text{ min}^{-1}$, $n = 3$). These values are significant because, in some cases, several measured rate constants are close in value, rendering the accuracy of one rate constant highly dependent upon another. For example, values of k_H , k_A and k_X for diethylphosphorylated AChE are almost identical in D₂O. The rate constants most sensitive to these equivalencies are the k_A values in Table 1. These values were obtained by fitting Equation (3), where the exponential rate constant is $k_A + k_X$. Therefore, from the $40 \times 10^{-6} \text{ min}^{-1}$ value of k_A in

Table 1, a 2-fold increase in k_X renders k_A close to zero. The value of k_X also plays an important, although lesser, role in the determination of k_H for diethylphosphorylated AChE in D₂O (Table 1 and Figure 4): a 2-fold increase in the fixed value of k_X in Equation (2) increases k_H by 45%, whereas a 2-fold decrease in k_X decreases k_H by 20%. Values of k_H , k_A , and k_X for dimethylphosphorylated AChE diverge to a much greater extent (see Table 1), making their accuracy largely independent of each other. In view of these differences in the rate constant interdependence of k_A and k_H , the similarities in the solvent D₂O isotope effects for dimethyl- and diethylphosphorylated AChE in Table 1 are reassuring but possibly serendipitous.

Table 1. Rate constants for reactions of organophosphorylated AChE and their solvent D₂O isotope effects.

Phosphoryl Substituents	Reaction	k (10^{-6} min^{-1}) H ₂ O ^a	k (10^{-6} min^{-1}) D ₂ O	n	$k \text{ H}_2\text{O}/k \text{ DO}$ ^b
Dimethyl- Diethyl-	Aging (k_A)	1500 ± 500	1400 ± 500	2	1.1 ± 0.1
		39 ± 7 ^c	41 ± 4 ^c	1	1.0 ± 0.2
Dimethyl- Diethyl-	Hydrolysis (k_H)	6000 ± 530	3100 ± 360	2	1.9 ± 0.1
		83 ± 12	41 ± 5	3	2.0 ± 0.1
Dimethyl- Diethyl-	2-PAM reactivation (k_R)	120,000 ± 6000	61,000 ± 4000	2	1.96 ± 0.04
		23,000 ± 1500	15,000 ± 300	2	1.68 ± 0.14

^a Values listed for rate constants k in H₂O are means of n experiments with the standard error of the mean. Since each entry in this table included paired measurements in H₂O and D₂O, n values were always the same for both solvents.

^b The solvent D₂O isotope effect was the ratio of a rate constant in H₂O to that in D₂O. It was the unweighted average of the isotope effects from the n experiments calculated individually for paired H₂O and D₂O reactions in each experiment. When $n = 1$, the standard error was determined from the combined errors of the H₂O and D₂O fits to Equation (3). ^c When $n = 1$, the standard error was determined from the error of the fit to Equation (3). However, the overall errors in k_A for diethylphosphorylated AChE depend much more on the values of k_X and k_H than on replicate values of k_A (see Section 2.5), and therefore replicate values of k_A for these species were not made.

2.6. Solvent Deuterium Oxide Isotope Effects on Reaction Rate Constants

Analyses of isotope effects in D₂O relative to H₂O have been useful in clarifying details of the AChE reaction pathway with a variety of substrates [15,16], but we've found few reports of these isotope effects on the reactions of phosphorylated AChE. In our experiments in this report, we paired rate constant determinations in H₂O and D₂O by running them on the same day, starting with the same stock AChE frozen aliquot and employing the same dilution sequence. Our results are presented in Table 1, and they are examined in detail in the Discussion.

3. Discussion

3.1. Kinetics of Decarbamylation and of the Hydrolysis of Organophosphorylated AChE

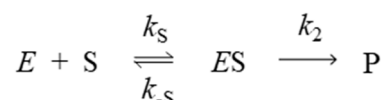
Rate constants for organophosphorylated AChE in Table 1 are in reasonable agreement with corresponding values previously reported in slightly different solvents, pH conditions and temperatures. Values of $k_A = 3000 \times 10^{-6} \text{ min}^{-1}$, of $k_H = 17,000 \times 10^{-6} \text{ min}^{-1}$, and of $k_R = 480,000 \times 10^{-6} \text{ min}^{-1}$ were obtained for dimethylphosphorylated human AChE [17]. For diethylphosphorylated AChE, values of $k_A = 170 \times 10^{-6} \text{ min}^{-1}$ and of $k_H = 120 \times 10^{-6} \text{ min}^{-1}$ were obtained with the mouse enzyme [18] and of $k_R = 60,000 \times 10^{-6} \text{ min}^{-1}$ for the human enzyme [19].

An increase in size of the carbamoyl or organophosphoryl group attached to AChE significantly reduced the value of k_3 or k_H for deacylation. In Table 1, the k_H for diethylphosphorylated AChE is about 75-fold lower than that for dimethylphosphorylated AChE. A similar trend was seen with carbamoylated AChE, where k_3 for *N,N*-diethylcarbamoyl AChE was about 300-fold lower than that for *N,N*-dimethylcarbamoyl AChE [2]. The difference for the organophosphorylated AChEs may result from distortion of the AChE active site by the larger diethylphosphoryl group as seen in Figure 2A. The organophosphoryl group size appears less important for oxime reactivation, as k_R in Table 1 for 2-PAM reactivation of diethylphosphorylated AChE is only 5-fold lower than that for

dimethylphosphorylated AChE. To address the consequences of active site distortion more directly, we analyzed the solvent D₂O isotope effects in the following section.

3.2. Solvent Deuterium Oxide Isotope Effects on Rate Constants for Reactions of Organophosphorylated AChE

When proton transfer occurs in the rate-limiting step of a reaction, the rate constant for that reaction shows a solvent D₂O isotope effect. Rate-limiting proton transfer in an acylation or deacylation reaction results in a rate constant decrease of 2 to 3-fold when D₂O replaces H₂O as the solvent [20]. AChE-catalyzed acetylcholine hydrolysis falls well within this range, as k_{cat} (a combination of acylation and deacylation rate constants) has a solvent D₂O isotope effect of 2.4 [15,21]. However, the isotope effect drops from 2.4 for k_{cat} to 1.1–1.2 for the second order hydrolysis rate constant $k_{\text{cat}}/K_{\text{app}}$ (also denoted k_{E}) with good substrates of AChE like acetylcholine. To interpret this drop, we proposed that proton transfer in the acylation step k_2 was rate-limiting for k_{cat} but that an earlier step like substrate binding, or an induced-fit conformational change that does not involve proton transfer, was rate-limiting for the second order rate constant $k_{\text{cat}}/K_{\text{app}}$ [15]. More explicitly, the solvent D₂O isotope effect is determined by the commitment to catalysis, denoted C [16]. In the very simple case of Scheme 3 and Equation (1), acetylcholine (S) binds to enzyme E with an association rate constant of k_{S} and a dissociation rate constant of $k_{-\text{S}}$ to give an ES complex.



Scheme 3. Pathway for hydrolysis of acetylthiocholine (S) by AChE (E).

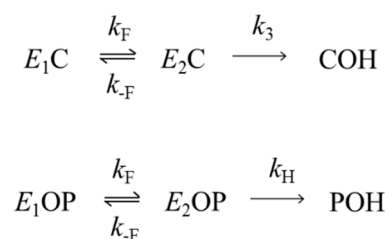
Subsequent acylation with a rate constant k_2 gives an acyl enzyme and choline products, here just denoted P. The observed rate constant k_{E} is given by Equation (1). The acylation step k_2 involves proton transfer and has an isotope effect of 2–3, while k_{S} and $k_{-\text{S}}$ are assumed not to involve proton transfer. The commitment to catalysis is defined as $C = k_2/k_{-\text{S}}$. When C is small, $k_{\text{E}} = k_{\text{S}} k_2/k_{-\text{S}}$, and k_{E} shows an isotope effect. When C is large, $k_{\text{E}} = k_{\text{S}}$ and it does not.

$$k_{\text{E}} = \frac{k_{\text{S}}k_2}{(k_{-\text{S}} + k_2)} \quad (1)$$

A comparable interpretation may be applied to the aging reaction in Scheme 2. This reaction is enzyme catalyzed [22] and involves loss of an alkyl group as the organophosphoryl adduct is converted from a phosphate triester to a diester. While a proton is transferred to the alkyl leaving group in this reaction, this transfer does not appear to be rate limiting as the solvent D₂O isotope effects for the aging reaction rate constant k_{A} in Table 1 are about 1.0. We have found no other reports of isotope effects on aging of dimethyl- or diethylphosphorylated AChE, but a similar isotope effect of 1.2 has been reported for aging of 2-propoxy-methylphosphonylated AChE [23].

We next asked whether the hydrolysis and oxime reactivation reactions in Scheme 2 involve general acid-base catalysis with rate-limiting proton transfer. To facilitate the analysis, we consider Scheme 4, which shows a slight extension of Scheme 1 in which a second acyl enzyme species is added in conformational equilibrium with the first. In particular, Scheme 4 includes an inactive enzyme form ($E_1\text{C}$ or $E_1\text{OP}$) with a distorted active site and an active enzyme form ($E_2\text{C}$ or $E_2\text{OP}$) that can undergo hydrolysis with a rate constant k_3 or k_{H} . The forward and reverse rate constants for these equilibria are k_{F} and $k_{-\text{F}}$, respectively, and they are assumed not to involve proton transfer. The general solution to Scheme 4 is more complicated than that of Scheme 3, as neither $E_2\text{C}$ nor $E_2\text{OP}$ necessarily is in the steady state. However, two extreme cases may be considered in which these intermediates are in the steady state: (1) the commitment to catalysis $k_3/k_{-\text{F}}$ or $k_{\text{H}}/k_{-\text{F}}$ is small, and the deacylation rate constant $k_3k_{\text{F}}/(k_{-\text{F}}+k_3)$ or $k_{\text{H}}k_{\text{F}}/(k_{-\text{F}}+k_{\text{H}})$ shows the solvent D₂O isotope effect inherent in k_3 or k_{H} ; (2) the commitment to catalysis $k_3/k_{-\text{F}}$ or $k_{\text{H}}/k_{-\text{F}}$ is large, the acyl intermediates are not equilibrated and

the deacylation rate constant $k_3k_F/(k_{-F}+k_H)$ or $k_Hk_F/(k_{-F}+k_H)$ shows only a fraction of the isotope effect inherent in k_3 or k_H and no isotope effect if k_3 or $k_H \gg k_{-F}$.



Scheme 4. Extension of Scheme 1 to include an inactive enzyme form (E_1C or E_1OP).

We recently investigated the hydrolysis of carbamoylated AChEs for a series of carbamate esters and obtained the solvent D_2O isotope effects summarized in Figure 6 [2]. The rate constant k_3 for the smallest carbamoyl group, an *N*-monomethylcarbamoyl, was $12 \times 10^{-3} \text{ min}^{-1}$, and its isotope effect of 2.8 was consistent with rate-limiting proton transfer and a small value of *C*. However, as the *N*-alkyl groups on carbamoylated AChEs increased in size, the decarbamoylation rate constant k_3 decreased to about $0.02 \times 10^{-3} \text{ min}^{-1}$ for *N,N*-diethylcarbamoylated AChE and the isotope effect was only slightly above 1 (Figure 6), indicating a high value of *C*. In that report we noted the crystallographic evidence of active site distortion in diethylphosphorylated AChE shown in Figure 2A, and we suggested that a larger size of the carbamoyl group is likely to be an important factor in a shift away from proton transfer in the rate-limiting step for k_3 . It may be useful to explore molecular modeling of the array of conformational variants available in AChEs with large carbamoyl groups to obtain support for this proposal.

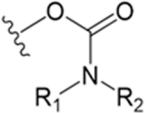
		Carbamoyl Substituents	$k_3 \text{H}_2\text{O} / k_3 \text{D}_2\text{O}$
R_1	R_2		
CH ₃	H	<i>N</i> -monomethyl	2.8 ± 0.2
CH ₃	CH ₃	<i>N,N</i> -dimethyl	2.4 ± 0.2
C ₂ H ₅	CH ₃	<i>N</i> -ethyl- <i>N</i> -methyl	1.8 ± 0.2
C ₂ H ₅	C ₂ H ₅	<i>N,N</i> -diethyl	1.1 ± 0.2

Figure 6. Solvent D_2O isotope effects on the AChE decarbamoylation rate constant k_3 at 25 °C [2].

We designed the experiments here to examine whether active site distortion in diethylphosphorylated AChE in fact does result in a shift away from rate-limiting proton transfer in the hydrolysis and oxime reactivation reactions of this AChE intermediate. For comparison, we included measurements of solvent D_2O isotope effects for dimethylphosphorylated AChE, an intermediate unlikely to involve active site distortion [10,12]. Oxime reactivation, like hydrolysis in Scheme 2, involves attack of a nucleophile on the tetravalent phosphorus to presumably form a pentavalent transition state [24]. This state then decomposes to regenerate active enzyme and an organophosphorylated oxime [7,25], and both the formation and decomposition of this state are likely to involve rate-limiting proton transfer. In the structure in Figure 2B, 50 mM 2-PAM was diffused into the crystal [9]. This structure suggests that 2-PAM stabilizes the active E_2OP species in Scheme 4, perhaps to the exclusion of the distorted E_1OP species, and k_R for diethylphosphorylated AChE in Table 1 is only 5-fold lower than that for dimethylphosphorylated AChE. These observations suggest that the concentration of E_1OP bound to 2-PAM is negligible and that k_R will reflect the rate-limiting proton transfer inherent when

both acyl groups migrate to the oxime. The solvent D₂O isotope effects of 2.0 and 1.7 for the dimethyl- and diethylphosphorylated AChE are consistent with this interpretation.

Finally, we examined the rate constants k_H for hydrolysis of both diethylphosphorylated AChE and dimethylphosphorylated AChE to determine if their solvent D₂O isotope effects reflect the fact that only diethylphosphorylated AChE appears to form the distorted active conformation in Figure 2A. The values in Table 1 do not support this proposal, as both organophosphorylated species show isotope effects that are close to 2.0. This value, although somewhat low for typical enzyme deacylation, suggests that any distorted conformation E_1OP involving diethylphosphorylated AChE equilibrates relatively rapidly with the active conformation E_2OP and that the commitment to catalysis $C = k_H/k_{-F}$ is small. These isotope effects for organophosphorylated AChE hydrolysis are significant because this reaction, of those in Scheme 2, bears the closest resemblance to the hydrolysis of the carbamoylated enzymes in Figure 6. Furthermore, the conclusion above that the commitment to catalysis $C = k_3/k_{-F}$ is large for *N,N*-diethylcarbamoylated AChE while $C = k_H/k_{-F}$ is small for diethylphosphorylated AChE is difficult to justify. Their respective rate constants, $k_3 = 0.02 \times 10^{-3} \text{ min}^{-1}$ for decarbamylation and $k_H = 0.08 \times 10^{-3} \text{ min}^{-1}$ for dephosphorylation (Table 1 and Figure 6), are too similar to support these opposing conclusions about C if the same value of k_{-F} holds for both acylated AChEs.

4. Materials and Methods

4.1. Reagents

Recombinant hAChE was expressed as a secreted, disulfide-linked dimer in drosophila S2 cells and purified by affinity chromatography as outlined previously [26]. Initial 0.5 mL fractions were maintained in 5 mM decamethonium bromide (Sigma-Aldrich Chemical Co., St. Louis, MO, USA) at 4 °C. Fractions were dialyzed against 20 mM sodium phosphate and 0.02% Triton X-100 (pH 7.0) at 4 °C, and 10- or 20- μL aliquots of the dialyzates were frozen at -20 °C until use. *O,O*-Diethyl *O*-(4-nitrophenyl) phosphate (paraoxon) and *O,O*-dimethyl *O*-(4-nitrophenyl) phosphate (paraoxon methyl) were commercial samples from Sigma-Aldrich Chemical Co (St. Louis, MO, USA).

4.2. Assay of Substrate Hydrolysis

Hydrolysis rates v for the substrate acetylthiocholine were measured in a coupled Ellman reaction in which thiocholine generated in the presence of the indicated concentration of DTNB was determined by the formation of the thiolate dianion of DTNB at 412 nm ($\Delta\epsilon_{412 \text{ nm}} = 14,150 \text{ M}^{-1}\text{cm}^{-1}$) [27]. Total AChE concentrations (E_{tot}) could be calculated assuming 450 units/nmol [28]. One unit of AChE activity corresponds to 1 μmol of acetylthiocholine hydrolyzed/min under standard pH-stat assay conditions at pH 8 [28,29]. Our conventional spectrophotometric assay at 412 nm was conducted in pH 7.0 buffer. With wild type hAChE and 0.5 mM acetylthiocholine, this assay resulted in 4.8 $\Delta A_{412 \text{ nm}}/\text{min}$ with 1 nM AChE or about 76% of the pH stat assay standard, but here E_{tot} was expressed simply in terms of $\Delta A_{412}/\text{min}$. The assay mixture here contained final concentrations of acetylthiocholine and DTNB of 1.0 mM and 0.3 mM, respectively, in 100 mM sodium phosphate and 0.1% BSA at pH 8.0. Aliquots of AChE were added to a final volume was 3.0 mL, and the assay was conducted at 25 °C. Absorbance at 412 nm was recorded with time on a Varian Cary 3A spectrophotometer.

4.3. Reactions of Organophosphorylated hAChE

We generated organophosphorylated AChE (EOP in Scheme 1) from either paraoxon (to give diethylphosphorylated AChE) or paraoxon methyl (to give dimethylphosphorylated AChE) as outlined in the legends to Figures 3–5. Experimental traces of organophosphorylated AChE reactions measured with acetylthiocholine activity assays (v) were obtained and the equation for the general solution used to fit these traces to Scheme 2 is given in Equation (2). Data were fitted to Equation (2) by unweighted

nonlinear regression with SigmaPlot (version 12.0, Systat Software Inc., Chicago, IL, USA). When $k_r \gg k_H + k_A + k_X$ and $t = t_{\text{aged}} \gg k_r^{-1}$, Equation (2) reduces to Equation (3).

$$v = \left(E_{\text{tot}} e^{-k_A t_{\text{aged}}} - E_0 \right) \frac{(k_r + k_H) \left(e^{-k_X t} - e^{-(k_r + k_H + k_A + k_X)t} \right)}{(k_r + k_H + k_A)} + E_0 e^{-k_X t} \quad (2)$$

$$v = E_{\text{tot}} e^{-(k_A + k_X)t_{\text{aged}}} \quad (3)$$

In Equations (2) and (3), t_{aged} is the time that enzyme and OP were incubated prior to the start of the measured reaction, t is the duration in min of the measured reaction and E_0 is the initial enzyme concentration ($\Delta A_{412}/\text{min}$ at $t = 0$).

Values of the second order reactivation rate constants k_r were obtained at various 2-PAM concentrations that were run in parallel, and these values were analyzed with Equation (4) to obtain the maximal first order reactivation rate constant k_R at saturating concentrations of 2-PAM and the dissociation constant K_P for 2-PAM binding to organophosphorylated AChE.

$$k_r = \frac{k_R}{1 + \frac{K_P}{[2\text{-PAM}]}} \quad (4)$$

4.4. Solvent Deuterium Oxide Isotope Effects

Reactions of organophosphorylated AChE were conducted in 100 mM sodium phosphate and 0.1% BSA at pH 8.0. The pH was the uncorrected value read by the pH meter for both H₂O and D₂O buffers, and the pH of 8.0 (rather than more typical pH values of 7.0–7.4 for AChE studies) was selected to minimize enzyme pK_a differences [3] between H₂O and D₂O. Organophosphorylated AChE reactions in D₂O were paired with reactions in H₂O to maximize precision in comparing rates. While frozen stocks of AChE were in H₂O, all subsequent dilutions were identical in either H₂O or D₂O. The percentage H₂O in an assayed D₂O aging reaction mixture was 3%, and the maximum percentage in hydrolysis or oxime reactivation mixtures was 1%.

Funding: This research received no external funding.

Conflicts of Interest: The author declares no competing financial interests.

Abbreviations

AChE: acetylcholinesterase; BSA, bovine serum albumin; hAChE, human acetylcholinesterase; mAChE, mouse acetylcholinesterase; TcAChE, *Torpedo californica* acetylcholinesterase; DTNB, 5,5'-dithiobis-(2-nitrobenzoic acid); 2-PAM, 2-pyridinealdoxime methiodide.

References

- Rosenberry, T.L. Quantitative simulation of endplate currents at neuro-muscular junctions based on the reactions of acetylcholine with acetylcholine receptor and acetylcholinesterase. *Biophys. J.* **1979**, *26*, 263–290. [[CrossRef](#)]
- Venkatasubban, K.S.; Johnson, J.L.; Thomas, J.L.; Fauq, A.; Cusack, B.; Rosenberry, T.L. Decarbamylation of acetylcholinesterases is markedly slowed as carbamoyl groups increase in size. *Arch. Biochem. Biophys.* **2018**, *655*, 67–74. [[CrossRef](#)] [[PubMed](#)]
- Reiner, E.; Aldridge, W.N. Effect of pH on inhibition and spontaneous reactivation of acetylcholinesterase treated with esters of phosphorus acids and of carbamic acids. *Biochem. J.* **1967**, *105*, 171–179. [[CrossRef](#)] [[PubMed](#)]
- Fukuto, T.R. Mechanism of action of organophosphorus and carbamate insecticides. *Environ. Health Perspect.* **1990**, *87*, 245–254. [[CrossRef](#)]
- Myers, D.K. Studies on cholinesterase. 10. Return of cholinesterase activity in the rat after inhibition by carbamoyl fluorides. *Biochem. J.* **1956**, *62*, 556–563.

6. Froede, H.C.; Wilson, I.B. Acetylcholinesterase. In *The Enzymes*, 3rd ed.; Boyer, P.D., Ed.; Academic Press: New York, NY, USA, 1971; pp. 87–114.
7. Wilson, I.B. Acetylcholinesterase. XI. Reversibility of tetraethyl pyrophosphate inhibitor. *J. Biol. Chem.* **1951**, *190*, 111–117.
8. Rosenberry, T.L.; Cheung, J. Rate-limiting step in the decarbamylation of acetylcholinesterases with large carbamoyl groups. *Chem. Biol. Interact.* **2019**, *308*, 392–395. [[CrossRef](#)]
9. Franklin, M.C.; Rudolph, M.J.; Ginter, C.; Cassidy, M.S.; Cheung, J. Structures of paraoxon-inhibited human acetylcholinesterase reveal perturbations of the acyl loop and the dimer interface. *Proteins* **2016**, *84*, 1246–1256. [[CrossRef](#)]
10. Hörnberg, A.; Tunemalm, A.K.; Ekström, F. Crystal structures of acetylcholinesterase in complex with organophosphorus compounds suggest that the acyl pocket modulates the aging reaction by precluding the formation of the trigonal bipyramidal transition state. *Biochemistry* **2007**, *46*, 4815–4825. [[CrossRef](#)]
11. Millard, C.B.; Kryger, G.; Ordentlich, A.; Greenblatt, H.M.; Harel, M.; Raves, M.L.; Segall, Y.; Barak, D.; Shafferman, A.; Silman, I.; et al. Crystal structures of aged phosphonylated acetylcholinesterase: Nerve agent reaction products at the atomic level. *Biochemistry* **1999**, *38*, 7032–7039. [[CrossRef](#)]
12. Millard, C.B.; Koellner, G.; Ordentlich, A.; Shafferman, A.; Silman, I.; Sussman, J.L. Reaction products of acetylcholinesterase and VX reveal a mobile histidine in the catalytic triad. *J. Am. Chem. Soc.* **1999**, *121*, 9883–9884. [[CrossRef](#)]
13. Kovalevsky, A.; Blumenthal, D.K.; Cheng, X.; Taylor, P.; Radic, Z. Limitations in current acetylcholinesterase structure-based design of oxime antidotes for organophosphate poisoning. *Ann. N. Y. Acad. Sci.* **2016**, *1378*, 41–49. [[CrossRef](#)] [[PubMed](#)]
14. Michel, H.O.; Hackley, B.E.; Berkowitz, L.; List, G.; Hackley, E.B.; Gillilan, W.; Pankau, M. Ageing and dealkylation of soman (pinacolylmethylphosphonofluoridate)-inactivated eel cholinesterase. *Arch. Biochem. Biophys.* **1967**, *121*, 29–34. [[CrossRef](#)]
15. Rosenberry, T.L. Catalysis by acetylcholinesterase. Evidence that the rate-limiting step for acylation with certain substrates precedes general acid-base catalysis. *Proc. Natl. Acad. Sci. USA* **1975**, *72*, 3834–3838.
16. Quinn, D.M. Acetylcholinesterase: Enzyme structure, reaction dynamics, and virtual transition states. *Chem. Rev.* **1987**, *87*, 955–979. [[CrossRef](#)]
17. Worek, F.; Diepold, C.; Eyer, P. Dimethylphosphoryl-inhibited human cholinesterases: Inhibition, reactivation, and aging kinetics. *Arch. Toxicol.* **1999**, *73*, 7–14. [[CrossRef](#)]
18. Jennings, L.L.; Malecki, M.; Komives, E.A.; Taylor, P. Direct analysis of the kinetic profiles of organophosphate-acetylcholinesterase adducts by MALDI-TOF mass spectrometry. *Biochemistry* **2003**, *42*, 11083–11091. [[CrossRef](#)]
19. Grosfeld, H.; Barak, D.; Ordentlich, A.; Velan, B.; Shafferman, A. Interactions of oxime reactivators with diethylphosphoryl adducts of human acetylcholinesterase and its mutant derivatives. *Mol. Pharmacol.* **1996**, *50*, 639–649.
20. Bender, M.L.; Hamilton, G.A. Kinetic isotope effects of deuterium oxide on several α -chymotrypsin-catalyzed reactions. *J. Am. Chem. Soc.* **1962**, *84*, 2570–2576. [[CrossRef](#)]
21. Bender, M.L.; Clement, G.E.; Kezdy, F.J.; Heck, H.D.A. The correlation of the pH (pD) dependence and the stepwise mechanism of α -chymotrypsin-catalyzed reactions. *J. Am. Chem. Soc.* **1964**, *86*, 3680–3690. [[CrossRef](#)]
22. Qian, N.; Kovach, I.M. Key active site residues in the inhibition of acetylcholinesterases by soman. *FEBS Lett.* **1993**, *336*, 263–266. [[CrossRef](#)]
23. Kovach, I.M.; Bennet, A.J. Comparative study of nucleophilic am) enzymic reactions of 2-propyl methylphosphonate derivatives. *Phosphorus Sulfur Silicon Relat. Elem.* **1990**, *51*, 51–56. [[CrossRef](#)]
24. Wong, L.; Radic, Z.; Bruggemann, R.J.M.; Hosea, N.; Berman, H.A.; Taylor, P. Mechanism of oxime reactivation of acetylcholinesterase analyzed by chirality and mutagenesis. *Biochemistry* **2000**, *39*, 5750–5757. [[CrossRef](#)] [[PubMed](#)]
25. Luo, C.; Saxena, A.; Smith, M.; Garcia, G.; Radic, Z.; Taylor, P.; Doctor, B.P. Phosphoryl oxime inhibition of acetylcholinesterase during oxime reactivation is prevented by edrophonium. *Biochemistry* **1999**, *38*, 9937–9947. [[CrossRef](#)] [[PubMed](#)]

26. Mallender, W.D.; Szegletes, T.; Rosenberry, T.L. Organophosphorylation of acetylcholinesterase in the presence of peripheral site ligands: Distinct effects of propidium and fasciculin. *J. Biol. Chem.* **1999**, *274*, 8491–8499. [[CrossRef](#)] [[PubMed](#)]
27. Johnson, J.L.; Cusack, B.; Davies, M.P.; Fauq, A.; Rosenberry, T.L. Unmasking tandem site interaction in human acetylcholinesterase. Substrate activation with a cationic acetanilide substrate. *Biochemistry* **2003**, *42*, 5438–5452. [[PubMed](#)]
28. De Ferrari, G.V.; Mallender, W.D.; Inestrosa, N.C.; Rosenberry, T.L. Thioflavin T is a fluorescent probe of the acetylcholinesterase peripheral site that reveals conformational interactions between the peripheral and acylation sites. *J. Biol. Chem.* **2001**, *276*, 23282–23287. [[CrossRef](#)]
29. Rosenberry, T.L.; Scoggin, D.M. Structure of human erythrocyte acetylcholinesterase. Characterization of intersubunit disulfide bonding and detergent interaction. *J. Biol. Chem.* **1984**, *259*, 5643–5652.

Sample Availability: Not available.



© 2020 by the author. Licensee MDPI, Basel, Switzerland. This article is an open access article distributed under the terms and conditions of the Creative Commons Attribution (CC BY) license (<http://creativecommons.org/licenses/by/4.0/>).